EUROPEAN JOURNAL OF PHARMACEUTICAL SCIENCES 28 (2006) 325–335

available at www.sciencedirect.com

SCIENCE DIRECT®

journal homepage: www.elsevier.com/locate/ejps

In vitro evaluation of N-methyl amide tripeptidomimetics as substrates for the human intestinal di-/tri-peptide transporter hPEPT1

Rikke Andersen[a], *Carsten Uhd Nielsen*[a], *Mikael Begtrup*[b], *Flemming Steen Jørgensen*[c], *Birger Brodin*[a], *Sven Frokjaer*[a], *Bente Steffansen*[a,*]

[a] *Molecular Biopharmaceutics, Department of Pharmaceutics and Analytical Chemistry, The Danish University of Pharmaceutical Sciences, 2-Universitetsparken, DK-2100 Copenhagen, Denmark*

[b] *Medicinal Chemistry, Department of Medicinal Chemistry, The Danish University of Pharmaceutical Sciences, 2-Universitetsparken, DK-2100 Copenhagen, Denmark*

[c] *Biostructural Research, Department of Medicinal Chemistry, The Danish University of Pharmaceutical Sciences, 2-Universitetsparken, DK-2100 Copenhagen, Denmark*

ARTICLE INFO

Article history:
Received 24 November 2005
Received in revised form 22 February 2006
Accepted 21 March 2006
Published on line 28 March 2006

Keywords:
hPEPT1
PEPT1
Tripeptides
Tripeptidomimetics
Transepithelial transport
N-methyl amide isostere

Abbreviations:
Ψ, N-methyl amide isostere (Ψ[CONCH$_3$]); PCA, Principal Component Analysis; AP, apical; BL, basolateral; Sar, sarcosine/sarcosyl

ABSTRACT

Oral absorption of tripeptides is generally mediated by the human intestinal di-/tri-peptide transporter, hPEPT1. However, the bioavailability of tripeptides is often limited due to degradation in the GI-tract by various peptidases. The aim of the present study was to evaluate the general application of N-methyl amide bioisosteres as peptide bond replacements in tripeptides in order to decrease degradation by peptidases and yet retain affinity for and transport via hPEPT1. Seven structurally diverse N-methyl amide tripeptidomimetics were selected based on a principal component analysis of structural properties of 6859 N-methyl amide tripeptidomimetics. *In vitro* extracellular degradation of the selected tripeptidomimetics as well as affinity for and transepithelial transport via hPEPT1 were investigated in Caco-2 cells. Decreased apparent degradation was observed for all tripeptidomimetics compared to the corresponding natural tripeptides. However, affinity for and transepithelial transport via hPEPT1 were only seen for Gly-Sar-Sar, AsnΨ[CONCH$_3$]PheΨ[CONCH$_3$]Trp, and Gly-Sar-Leu. This implies that tripeptidomimetics originating from tripeptides with neutral side chains are more likely to be substrates for hPEPT1 than tripeptidomimetics with charged side chains. The results of the present study indicate that the N-methyl amide peptide bond replacement approach for increasing bioavailability of tripeptidomimetic drug candidates is not generally applicable to all tripeptides. Nevertheless, retained affinity for and transport via hPEPT1 were shown for three of the evaluated N-methyl amide tripeptidomimetics.

1. Introduction

Tripeptides with crucial physiological activities are potential lead compounds for drug discovery and development. The recently discovered tripeptides Tyr-Ser-Val (YSV) and Tyr-Ser-Leu (YSL) extracted from pig spleen may hold promising prospectives, since these tripeptides were reported to have an antitumor effect on human hepatocarcinoma in nude mice

* Corresponding author. Tel.: +45 3530221; fax: +45 35306030.
E-mail address: bds@dfuni.dk (B. Steffansen).

0928-0987/$ – see front matter © 2006 Elsevier B.V. All rights reserved.
doi:10.1016/j.ejps.2006.03.007

(Jia et al., 2005; Yao et al., 2005). In another study Gly-Pro-Arg was suggested to reduce neuronal cell death through inhibition of apoptosis in rat hippocampal neurons (Ioudina and Uemura, 2003). Likewise, the tripeptide aldehyde D-Phe-Pro-Arg-H derived from the thrombin cleavage site has been recognized as a core structure for the development of thrombin inhibitors (Lange et al., 2003).

The possibilities in using natural tripeptides as drug compounds are often very limited due to their instability in body fluids and tissues. Tripeptides are susceptible to hydrolysis in the GI-lumen as well as in the enterocytes. To exert their pharmacological activity, tripeptides must remain intact during the absorption process. Therefore, stabilization of the tripeptides is an obvious way to increase the bioavailability of such compounds. The strategy for stabilization could be to introduce unnatural amino acids, modifying the *N*- or *C*-termini or to introduce peptide bond bioisosteres.

Structural modifications of tripeptides might, however, influence their absorption in the small intestine. Natural tripeptides arising from food are substrates for the human di-/tri-peptide transporter, hPEPT1, which is localized in the luminal membrane of enterocytes (Liang et al., 1995). Therefore, this carrier may also play an important role in the absorption of tripeptidomimetic drugs. Thus, in the process of stabilizing tripeptides, an equally important requirement is to maintain affinity for and transport via hPEPT1.

The tripeptide-like β-lactam antibiotics are well-known examples of compounds where, retrospectively, the high oral bioavailability has been explained by a high resistance towards enzymatic degradation in the GI tract and an absorption partly due to transport via hPEPT1 across the intestinal epithelium (Bretschneider et al., 1999; Dantzig, 1998). Furthermore, several stabilization strategies yielding substrates for hPEPT1 are described in the literature, although, primarily applied on dipeptides. Transport via hPEPT1 of dipeptides containing a ketomethylene bioisosteres as peptide bond replacement has been shown for the aminopeptidase inhibitor arphamenine A (an Arg-Phe mimetic) (Enjoh et al., 1996), the photosensitizer δ-aminolevulinic acid (a Gly-Gly mimetic) (Doring et al., 1998), and a series of model dipeptidomimetica prodrugs as well as the dipeptidomimetica of Phe-Gly (Våbenø et al., 2004a, 2004b). The thioamide isostere, when introduced into Ala-Pro, is accepted by hPEPT1 (Brandsch et al., 1998). Gly-Sar, which contains a *N*-methyl amide isostere, is a well characterized standard substrate for hPEPT1. The corresponding tripeptide Gly-Sar-Sar (GΨGΨG) has also been suggested to be actively transported across the intestinal epithelium via peptide transporters when investigated in rings of everted hamster jejunum and in rat renal brush border membrane vesicles (Addison et al., 1975; Sleisenger et al., 1976; Daniel et al., 1992; Minami et al., 1992). Despite many examples of peptide bond replacements, the potential and general application of peptide bond bioisosteres such as *N*-methyl amide in relation to hPEPT-affinity and -mediated transport has not yet been systematically investigated.

In the present study our aim was to evaluate the general application of *N*-methyl amide isosteres as peptide bond replacements in tripeptides to decrease degradation by peptidases and yet retain affinity for and transport via hPEPT1. The affinity for and transport via hPEPT1 were studied for a series of *N*-methyl amide tripeptidomimetics using Caco-2 cell monolayers.

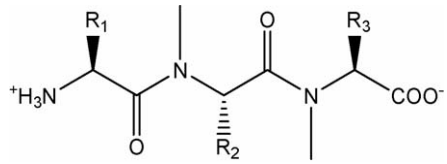

Fig. 1 – The general structure of *N*-methyl amide tripeptidomimetics. R_1, R_2, and R_3 are side chains originating from naturally occurring amino acids except proline.

The evaluated tripeptidomimetics were selected in order to represent the structural diversity among all possible *N*-methyl amide tripeptidomimetics constructed from natural amino acids (Fig. 1). Recently, we reported the successful use of VolSurf descriptors when describing the diversity in structural properties of tripeptides, and how these structural properties correlated well with the affinity for hPEPT1 (Andersen et al., 2006). Therefore, VolSurf descriptors were generated for all possible *N*-methyl amide tripeptidomimetics. Based on a principal component analysis (PCA) of the molecular descriptors, the structural property space spanned by the 6859 tripeptidomimetics was created. The evaluated tripeptidomimetics were selected to cover as much of the variation in structural properties as possible, yet limiting the number of compounds to be synthesized and investigated. This compound selection approach enables a general evaluation of *N*-methylated tripeptides with regard to *In vitro* apparent degradation and affinity and transport via hPEPT1.

2. Materials and methods

2.1. *Materials and apparatus*

H-LysΨ[CONCH$_3$]TrpΨ[CONCH$_3$]Arg-OH (KΨWΨR) (purity >95%), H-AspΨ[CONCH$_3$]ArgΨ[CONCH$_3$]Glu-OH (DΨRΨE) (purity >99%), H-GlyΨ[CONCH$_3$]GluΨ[CONCH$_3$]Trp-OH (GΨEΨW) (purity >97%), and H-AsnΨ[CONCH$_3$]PheΨ[CONCH$_3$]Trp-OH (NΨFΨW) (purity >98%) were custom synthesized as TFA salts by BaChem (Weil am Rhein, Germany). H-Lys-Trp-Arg-OH (KWR), H-Asp-Arg-Glu-OH (DRE), and H-Asn-Phe-Trp-OH (NFW) were custom synthesized as TFA salts with HPLC purity >98% at SynPep (Dublin, California). H-Gly-Glu-Trp-OH (GEW) was custom synthesized as TFA salts with HPLC purity >99% at NeoSystem (Strasbourg, France). H-Gly-Sar-Sar-OH (GΨGΨG), H-Gly-Gly-Gly-OH (GGG) (purity >99%), H-Gly-Gly-Leu-OH (GGL) (purity >99%), and H-Gly-Phe-Gly-OH (GFG) (purity >98%) were purchased at BaChem AG (Weil am Rhein, Germany). Proper characterization and proof of structure was provided by the manufacturer. H-GlyΨ[CONCH$_3$]Phe-Sar-OH (**7**) (GΨGΨL) and H-Gly-Sar-Ψ[CONCH$_3$]Leu-OH (**12**) (GΨFΨG) were prepared and characterized as described below. Structures of H-Gly-SarΨ[CONCH$_3$]Leu-OH and H-GlyΨ[CONCH$_3$]Phe-Sar-OH were verified by ^{1}H and ^{13}C NMR spectra recorded on a 300 MHz instrument. Chemical shifts are given in ppm (δ-values)

relative to the internal standard tetramethylsilane (TMS). The ^{1}H NMR spectra were assigned by comparison with spectra of the individual amino acids. In many cases, marked with an asterix, both E- and Z-conformers, due to restricted rotation around the amide C–N bond, could be observed. Elemental analyses were performed by Microanalytical Laboratory, Department of Physical Chemistry, University of Vienna, Austria.

Caco-2 cells were obtained from the American Type Culture Collection (Manassas, Virginia). Cell culture media and Hanks balanced salt solution (HBSS) were obtained from Life Technologies (Høje Taastrup, Denmark). Phosphate-buffered saline (PBS) was purchased from BioChrom AG (Berlin, Germany). All solvents were of analytical grade, and chemicals used in buffer preparations were of laboratory grade. Trifluoroacetic acid (TFA), 1-octanesulfonic acid (OSA), 2-[*N*-morpholino]ethanesulfonic acid (MES) and *N*-[2-Hydroxyethyl]piperazine-*N*′-2-ethanesulfonic acid (HEPES), bovine serum albumin (BSA), δ-aminolevulinic acid, H-Gly-Pro-OH, Triton X-100, and *N*,*N*-dimethylacetamide were from Sigma (St. Louis, MO, USA). [^{14}C]Gly-Sar and [^{3}H]mannitol, with specific activities of 49.94 and 51.50 mCi/mmol, respectively, were purchased from New England Nuclear (Boston, MA, USA). Chemicals used in the described syntheses were purchased from Sigma (St. Louis, MO, USA) or BaChem AG (Weil am Rhein, Germany) and used without further purification with the exceptions of dimethyl formamide (DMF) and dichloromethane (DCM), which were dried and stored over 3 Å molecular sieves. Chromatography was performed with matrex silica, 60A/35–70 μm (Millipore, Copenhagen, Denmark).

The HPLC system for quantitative analyses was a Merck Hitachi LaChrom Elite equipped with an autosampler (L-2300) with integrated cooling unit, a HTA pump (L-2130), a column own (L-2300), and a diode array detector (L-2450). The system was operated with Merck EZChrom Elite (v3.1.3) software. All compounds were eluted on a Waters Spherisorb S5OdS2 reversed-phase column (5 μm, 250 mm × 4.6 mm). Radioactivity was counted on a Tri-Carb 2110TR liquid scintillation analyzer from Packard (Perkin-Elmer Life and Analytical Sciences, Boston, MA).

The transepithelial electrical resistance (TEER) of Caco-2 cell monolayers was measured in a tissue resistance measurement chamber (Endohm) with a voltohmmeter (EVOM) from World Precision Instruments (Sarasota, FL, USA). The shaking plate used for cell culture experiments was a Swip KS 10 Digi from Edmund Bühler (Hechingen, Germany).

2.2. *Synthesis of H-Gly-SarΨ[CONCH$_3$]Leu-OH (12) and H-GlyΨ[CONCH$_3$]Phe-Sar-OH (7)*

All reactions involving air-sensitive reagents were performed under nitrogen. All glassware was flame-dried prior to use. *N*-(3-Dimethylaminopropyl)-*N*′-ethylcarbodiimide hydrochloride (EDAC) was handled under a nitrogen atmosphere as previously described (Friedrichsen et al., 2001). The crude products were purified by flash chromatography (Still et al., 1978).

The procedure for peptide coupling between *N*-methylated amino acids is illustrated by the following procedure and a schematic outline is presented in Scheme 1. Boc-GlyΨ[CONCH$_3$]Phe-OH (**4**), (200 mg, 0.59 mmol), Sar-OBn, tosylate (**5**) (186 mg, 0.53 mmol), 1-hydroxybenzotriazole hydrate (91 mg, 0.59 mmol), EDAC (170 mg. 0.89 mmol), DMF (1.5 ml), and diisopropylethylamine (0.5 ml) were stirred under nitrogen for 20 h, the mixture was then evaporated to dryness in vacuo, extracted with boiling ethyl acetate (25 ml), washed with sat. aq NaCl (2 ml × 15 ml), sat. aq. $NaHCO_3$ (2 ml × 15 ml), 10% aq. citric acid (2 ml × 20 ml), and sat. aq. NaCl (1 ml × 15 ml), dried on $MgSO_4$. After filtration, the ethyl acetate was removed in vacuo and followed by flash chromatography (ethyl acetate–heptane 1:2). The yield was 200 mg (76%) of Boc-GlyΨ[CONCH$_3$]Phe-Sar-OBn (**6**) as an oil, rf 0.10 (ethyl acetate–heptane 1:2). δ_H ($CDCl_3$) 7.29–7.10 (10H, m, 2 Ph), 5.68–5.58 (1H, m, CH in Phe), 5.04 (2H, m, CH_2 in Bn), 4.32–.57 (4H, m, CH_2 in Gly and Sar), 3.14–2.77 (2H, m, CH_2 in Phe), 2.77–2.92 (6H, m, 2NCH_3), 1.36 and 1.31* (9H, s, $(CH_3)_3$). *Two conformers.

The benzyl and Boc protecting groups were removed by dissolving Boc-GlyΨ[CONCH$_3$]Phe-Sar-OBn (**6**) (0.18 g, 0.36 mmol) in ethyl acetate (30 ml). 10% Palladium on carbon (300 mg) was added, and the solution was stirred under hydrogen for 16 h. Filtration, extraction with further 100 ml of ethyl acetate and evaporation to dryness gave 90 mg (61%) Boc-GlyΨ[CONCH$_3$]Phe-Sar-OH as an oil, rf 0.09 (ethyl acetate). The crude product (85 mg, 0.21 mmol) was dissolved in dichloromethane (25 ml). After addition of TFA (12.5 ml), the solution was stirred for 3 h. The solvent was removed in vacuo. Co-evaporation with chloroform (3 ml × 3 ml) yielded 90 mg (100%) of semi-solid H-GlyΨ[CONCH$_3$]Phe-Sar-OH, trifluoroacetate (**7**). δ_H (CD_3OD) 7.26–7.20 (5H, m, Ph from Phe), 5.78–5.65

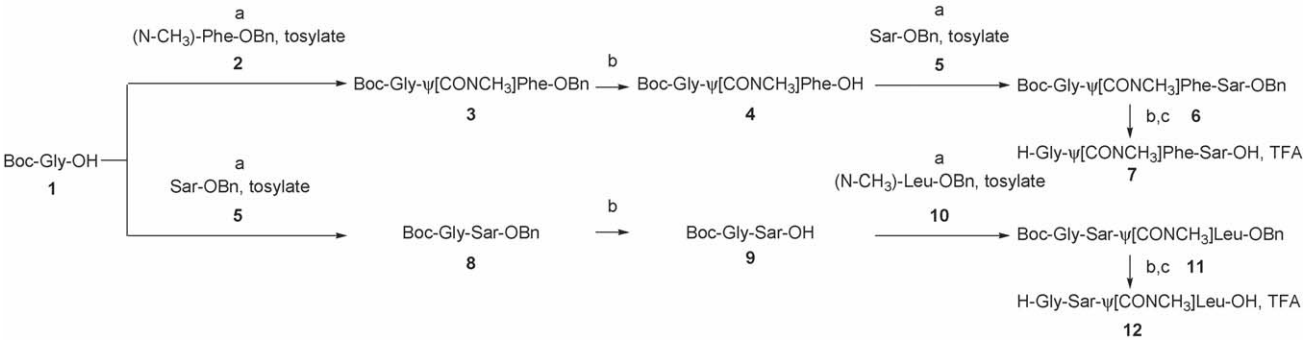

Scheme 1 – Synthesis of tripeptides 7 and 12. (a) Coupling conditions given in Section 2.2, (b) H_2 Pd/C, (c) TFA.

(1H, m, CH in Phe), 4.28–3.73 (4H, m, CH_2 in Gly and Sar), 3.22–3.03 (2H, m, CH_2 in Phe), 3.03–2.93 (6H, m, $2NCH_3$).

Using these procedures, coupling of Boc-Gly-OH (**1**) and (*N*-methyl)-Phe-OBn, tosylate (**2**) afforded Boc-Gly Ψ[$CONCH_3$]Phe-OBn (**3**), rf 0.35 (ethyl acetate–heptane 1:2). δ_H ($CDCl_3$) 7.32–7.13 (10H, m, 2Ph), 5.21 (1H, m, CH in Phe), 5.10 (2H, m, CH_2 in Bn), 3.86–3.65 (2H, m, CH_2 in Gly), 3.35–2.98 (2H, m, CH_2 in Phe), 2.82 and 2.67* (3H, m, NCH_3 in (*N*-methyl)-Phe), 1.36 and 1.34* (9H, s, $(CH_3)_3$). Anal. calc. for $C_{24}H_{30}N_2O_5$: C, 67.59; H, 7.09; N, 6.57. Found: C, 67.84; H, 6.92; N, 6.48. Debenzylation produced Boc-GlyΨ[$CONCH_3$]Phe-OH (**4**), rf 0.04 (ethyl acetate-heptane 1:2) which was used without further purification in the next step. *Two conformers.

Similarly, coupling of Boc-Gly-OH (**1**) and Sar-OBn, tosylate (**5**) gave Boc-Gly-Sar-OBn (**8**), rf 0.06 (ethyl acetate–heptane 1:3). Debenzylation produced Boc-Gly-Sar-OH (**9**), rf 0.08 (ethyl acetate) which was used without further purification in the next step where coupling of Boc-Gly-Sar-OH (**9**) and (*N*-methyl)-Leu-OBn, tosylate (**10**) gave Boc-Gly-SarΨ[$CONCH_3$]Leu-OBn (**11**), rf 0.67 (ethyl acetate), δ_H ($CDCl_3$) 7.31 (5H, m, Ph), 5.39 and 5.25* (1H, m, CH in Leu), 5.08 (2H, m, CH_2 in Bn), 4.35–3.95 (4H, m, 2 CH_2 in Gly and Sar), 2.92 and 2.82* (6H, m, 2 NCH_3), 1.68 (3H, m, CH and CH_2 in Leu), 1.38 (9H, s, $(CH_3)_3$), 0.86 (6H, m, 2 CH_3 in Leu), anal. calc. for $C_{24}H_{37}N_3O_6$: C, 62.18; H, 8.04; N, 9.06. Found: C, 61.90; H, 7.77; N, 9.34. Debenzylation produced Boc-Gly-SarΨ[$CONCH_3$]Leu-OH, rf 0.02 (ethyl acetate). Subsequent removal of the Boc-group gave H-Gly-SarΨ[$CONCH_3$]Leu-OH, trifluoroacetate (**12**), δ_H (CD_3OD), 5.15 (1H, m, CH in Leu), 4.44–3.77 (4H, m, CH_2 in Gly and Sar), 2.98–2.83* (6H, m, $2NCH_3$), 1.78–1.51 (3H, m, CH and CH_2 in Leu), 0.97–0.90 (6H, m, 2 CH_3 in Leu). *Two conformers.

The HPLC purity of H-Gly-SarΨ[$CONCH_3$]Leu-OH (**12**) and H-GlyΨ[$CONCH_3$]Phe-Sar-OH (**7**) was >96% and >94%. The compounds will be referred to as GΨGΨL and GΨFΨG, respectively.

2.3. Biological investigations

2.3.1. Cell culture

Caco-2 cells were cultured as previously described (Nielsen et al., 2001a). Briefly, cells were seeded in culture flasks and passaged in Dulbecco's Modified Eagle's medium (DMEM) supplemented with 10% fetal bovine serum, penicillin/streptomycin (100 U/ml and 100 μg/ml, respectively), 1% L-glutamine, and 1% nonessential amino acids. Caco-2 cells were seeded onto tissue culture treated 12-well Transwell plates (1.13 cm^2, 0.4 μm pore size) at a density of 10^5 cells × cm^{-2}. Monolayers were grown in an atmosphere of 5% CO_2–95% O_2 at 37 °C. Growth media were replaced every other day. TEER was measured at room temperature before each experiment. The monolayers used had TEER's in the range of 400–700 Ω cm^{-2}. Experiments were performed on day 25–27 after seeding. Caco-2 cell from passages 21–48 were used for the experiments.

2.3.2. Affinity measurements

Affinity for hPEPT1 of tripeptidomimetics was measured as concentration-dependent inhibition of apical [^{14}C]Gly-Sar (20 μM) uptake in Caco-2 cell monolayers as described by Nielsen et al. (2001b). In brief, Caco-2 cells were equilibrated for 15 min with 0.5 ml buffer pH 6.0 (HBSS supplemented with 10 mM MES and 0.05% BSA) on the apical (AP) side and 1 ml buffer pH 7.4 (HBSS supplemented with 10 mM HEPES and 0.05% BSA) on the basolateral (BL) side. After 15 min, the buffers were removed and solutions of 20 μM (1 μCi/ml) [^{14}C]Gly-Sar with varying concentrations of GΨGΨG, GΨGΨL, GΨFΨG, NΨFΨW, GΨEΨW, DΨRΨE or KΨWΨR (0–10 mM) in buffer adjusted to pH 6.0 were added to the AP side, and buffer pH 7.4 was added to the BL side of the monolayers. The aqueous solubility of GΨGΨL and GΨFΨG was increased by addition of 3% *N*,*N*-dimethylacetamide, which was shown to have no influence on the uptake of [^{14}C]Gly-Sar (data not shown). After 5 min, the solutions were removed and cells were washed with ice-cold HBSS buffer. The filter supports were cut out and the amount of [^{14}C]Gly-Sar was measured by liquid scintillation spectrometry. Experiments with Caco-2 cells were performed using at least four separate monolayers.

2.3.3. Transepithelial transport

The concentration-dependent AP to BL transepithelial transport was measured in the concentration range of 0.4–15 mM GΨGΨG (Gly-Sar-Sar) or 2–5 mM GΨGΨG in presence of 20 mM Gly-Pro in buffer pH 6.0. Accordingly, AP to BL transepithelial transport was measured for 2 mM GΨGΨG, NΨFΨW, GΨGΨL, or GΨFΨG in presence of 20 mM Gly-Pro in buffer pH 6.0. 3% *N*,*N*-dimethylacetamide were added to the solutions of GΨGΨL and GΨFΨG. The AP to BL transepithelial transport studies were performed by adding the various solutions of tripeptidomimetics to the AP side and buffer pH 7.4 to the BL side of the cell monolayers. Before the transport experiments, the Caco-2 cells were equilibrated for 15 min with 0.5 ml buffer pH 6.0 on the AP side and 1 ml buffer pH 7.4 on the BL side. After 15 min, buffers were removed and the AP to BL transport studies were initiated. AP donor samples (20 μl) were taken at 0, 60, and 140 min. BL receiver samples (100 μl) were taken at 60, 80, 100, 120, and 140 min and replaced with buffer pH 7.4.

Concentration-dependent BL to AP transepithelial transport of 2–10 mM GΨGΨG was initiated by addition of solutions in buffer pH 7.4 to the BL side and buffer pH 7.4 to the AP side. Before the experiments, the Caco-2 cells were equilibrated with buffer pH 7.4 on both AP and BL side for 15 min. AP receiver samples (25 μl) were taken at 60, 80, 100, 120, and 140 min and replaced with buffer pH 7.4. BL donor samples (20 μl) were taken at 0, 60, and 140 min.

All samples were transferred to HPLC vials and analyzed by HPLC-UV. The integrity of the Caco-2 cell monolayers were evaluated after the transport studies by measuring the [^{3}H]mannitol flux. The apparent permeability (P_{app}) of [^{3}H]mannitol typically ranged from 0.1×10^{-6} to 0.6×10^{-6} cm/s. Fluxes of the tripeptidomimetics were constant after 60 min.

2.3.4. Apical and basolateral uptake

Concentration-dependent AP uptake of GΨGΨG was measured at concentrations ranging from 0.5 to 10 mM. Solutions (0.5 ml) were adjusted to pH 6.0 in buffer and added to the AP side and 1 ml buffer pH 7.4 to the BL side. AP donor samples were taken every 20 min. The BL uptake experiments

were initiated by adding 20 mM GΨGΨG in absence or presence of 20 mM Gly-Pro in buffer pH 7.4 (pH adjusted) to the BL side and buffer pH 7.4 to the AP side of Caco-2 cells. BL donor samples were taken every 20 min. After 10 min AP or BL uptake experiment, solutions were removed and cells were washed with ice cold HBSS. Cells were detached from filters by adding 100 μl 0.1% Triton-X in PBS and incubating at 37 °C for 15 min. The cell suspensions were transferred to eppendorf tubes and frozen to −18 °C. Before analyzing, cell suspensions were thawed and centrifuged for 15 min, 4 °C, and 14000 rpm. The supernatants and donor samples were analyzed by HPLC-UV. The time dependent uptake AP to BL and BL to AP of 15 mM GΨGΨG was linear until 10 and 15 min, respectively.

2.3.5. *Apparent degradation*

The apparent degradation of the tripeptidomimetics, when exposed to extracellular peptidases, was estimated by adding the compounds to the AP side of Caco-2 cell monolayers. To limit uptake of the tripeptidomimetics during the experiment, an excess of a high affinity hPEPT1 substrate (δ-aminolevulinic acid (20 mM, K_i = 1.5 mM)) was added to the AP side. Depending on the K_i-value of the compounds, this resulted in more than 98% inhibition of uptake. The experiments were initiated by adding 0.5 ml of 0.5 mM tripeptidomimetic and 20 mM δ-aminolevulinic acid in buffer pH 6.0 to the AP side and 1 ml buffer pH 7.4 to the BL side of the Caco-2 cell monolayers. AP samples (20 μl) were taken at different time points (0–60 min), transferred to vials on ice and analyzed on HPLC-UV. The degradation of tripeptidomimetics was investigated in three separate experiments for each compound.

2.3.6. *Analytical HPLC methods*

All the developed HPLC methods kept a flow rate at 1 ml/min and an auto sampler temperature at 4 °C. The following mobile phases was used; GΨGΨG: 1% phosphoric acid, 10 mM 1-octanesulfonic acid, and 10% acetonitril (AcN); GΨGΨL and GΨFΨG: 0.05% TFA and 25% AcN; NΨFΨW: 20 mM acetate (pH 5), 0.05% TEA, and 30% AcN; KΨWΨR: 0.05% TFA and 10% AcN; GΨEΨW: 0.05% TFA and 20% AcN; DΨRΨE: 1% phosphoric acid, 10 mM 1-octanesulfonic acid, and 30% Acn. Column temperatures were 25–50 °C and the wavelength used in UV detection was 210 or 220 nm. Retention times ranged from 6.3 to 10.4 min.

2.4. *Molecular descriptors*

VolSurf descriptors were calculated using the VolSurf (v4.2.1) program implemented in SYBYL (v6.9.1). Cruciani et al. (2000) have extensively described the methodology behind the VolSurf descriptors. According to standard procedures, the VolSurf descriptors were based on GRID 3D molecular interaction fields (MIFs) resulting from interaction energies between the ligand and different probes. VolSurf descriptors were generated for a data set of 6859 N-methyl amide tripeptidomimetics (cf. Fig. 1), using the probes H_2O, DRY, and O. The tripeptidomimetics were built in SYBYL and protonated according to pH 6.0. The VolSurf descriptors were generated with default settings. For a detailed description of VolSurf descriptors cf. ref. VolSurf Manual (2005) and Cruciani et al. (2000).

2.5. *Data analysis*

2.5.1. *Transport kinetics*

The AP to BL transepithelial flux, J, of 2 mM GΨGΨG, GΨGΨL, NΨFΨW, and GΨFΨG in presence or absence of 20 mM Gly-Pro and the basolateral uptake of 20 mM GΨGΨG in presence or absence of 20 mM Gly-Pro were calculated as $J = \Delta Q/\Delta t/A$, where $\Delta Q/\Delta t$ is the accumulated amount of intact tripeptidomimetic on the receiver side, and A is the area of the Caco-2 cell monolayer (1.13 cm^2).

The BL to AP transepithelial transport of GΨGΨG and the AP to BL transepithelial transport of GΨGΨG in presence of Gly-Pro were non-saturable and apparent permeabilities (P_{app}) were determined by linear regression according to Fick's first law:

$$P_{app} = \frac{J}{C_0} \quad (1)$$

where C_0 is the initial concentration on the donor side.

The AP to BL transepithelial transport and apical uptake of GΨGΨG at various concentrations were saturable and fitted to a Michaelis–Menten-like expression:

$$J = \frac{J_{max}[S]^{n_H}}{K_m^{n_H} + [S]^{n_H}} \quad (2)$$

where J is the flux of the tripeptidomimetic, J_{max} the maximal flux, S the concentration of the tripeptidomimetic, K_m the Michaelis–Menten constant, and n_H is the Hill-constant.

Apparent affinity for hPEPT1 in Caco-2 cells was determined as concentration-dependent inhibition of [^{14}C]Gly-Sar uptake. The IC_{50}-values were calculated as described in Nielsen et al. (2001b) and the conversion of IC_{50} to K_i as described by Cheng and Prusoff (1973).

2.5.2. *Apparent degradation*

The apparent degradation of tripeptidomimetic was measured as the amount of intact compound on the apical side of Caco-2 cell monolayers. The apparent degradation was considered to be pseudo-first-order, thus calculated as

$$\%\,\text{intact tripeptidomimetic} = 100\% - (1 - e^{-k_{obs}t}) \times 100\% \quad (3)$$

where k_{obs} is the estimated pseudo-first-order rate constant and t is the time.

Tripeptidomimetics were excluded from the study if less than 90% of the compound was available as intact tripeptidomimetic on the AP side of the cell monolayers after 5 min (length of affinity assay). This 90% limit was assessed due to the influence degradation products (dipeptidomimetics) may exert on the interpretation of measured apparent binding affinities of the tripeptidomimetics.

2.5.3. *Multivariate data analysis*

The VolSurf descriptors were analyzed by PCA (Principal Component Analysis) in SIMCA-P (v10.0). Default settings were applied. The variables were centered and scaled to unit variance. Cross validation (seven rounds) was performed to test the significance of the model.

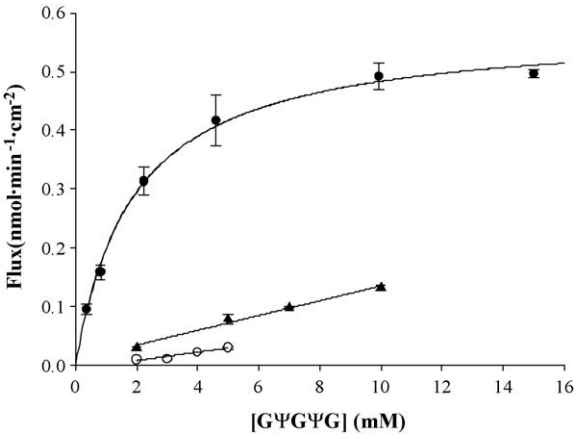

Fig. 2 – Transepithelial transport of GΨGΨG. Circles represent the apical to basolateral flux of GΨGΨG in absence (black) (N = 6) and presence (white) of 20 mM Gly-Pro (N = 3). Black triangles represents the basolateral to apical flux of GΨGΨG (N = 3). Data are given as mean ± S.E.M.

2.5.4. *Statistics*

The statistical significance of the results was determined using a two-tailed unpaired Students *t*-test. Affinity and transport experiments on Caco-2 cell monolayers were performed in multiple passages. *N* is the number of repetitions for each experiment, which in all experiments were ≥3. Experiments on apparent stability were performed in triplicates ($N = 3$). $p < 0.05$ was considered significant.

3. Results

3.1. *Transport mechanism of GΨGΨG*

The transepithelial transport and apical (AP) uptake mechanisms of GΨGΨG (Gly-Sar-Sar) were investigated to determine whether *N*-methyl amide tripeptidomimetics could be substrates for hPEPT1.

The AP to basolateral (BL) transport of GΨGΨG across Caco-2 cell monolayers was found to be saturable (Fig. 2). Data were fitted to Eq. (2), which gave the kinetic parameters listed in Table 1. In the presence of Gly-Pro, a hPEPT1 substrate, carrier-mediated AP to BL transport of GΨGΨG was abolished, and only a minor non-saturable flux component ($P_{app} = 1.2 \times 10^{-7} \pm 8.0 \times 10^{-9}$ cm s^{-1}) was observed (Fig. 2). BL to AP transport of GΨGΨG was non-saturable with a P_{app} of $2.0 \times 10^{-7} \pm 1.0 \times 10^{-8}$ cm s^{-1}, which was comparable to the non-saturable AP to BL transport.

The intracellular uptake of GΨGΨG from the AP side was saturable (Fig. 3, left) and data fitted nicely to the Michaelis–Menten equation (Eq. (2)), which gave the kinetic parameters listed in Table 1. The intracellular uptake of 20 mM GΨGΨG from the BL side was significantly inhibited by 20 mM Gly-Pro (Fig. 3, right). This inhibitable component was approximately 65% of the total GΨGΨG uptake.

Table 1 – Kinetic parameters for the transepithelial transport and apical uptake of GΨGΨG

Transport direction	Kinetic parameters[a]
AP to BL	$J_{max} = 0.55 \pm 0.02$ nmol min^{-1} cm^{-2} $K_m = 1.7 \pm 0.2$ mM $n_H = 1.1 \pm 0.1$
AP to BL (20 mM Gly-Pro)	$P_{app} = 1.2 \times 10^{-7} \pm 2.4 \times 10^{-8}$ cm s^{-1}
BL to AP	$P_{app} = 2.0 \times 10^{-7} \pm 1.7 \times 10^{-8}$ cm s^{-1}
AP to cytosol (uptake)	$J_{max} = 1.8 \pm 0.2$ nmol min^{-1} cm^{-2} $K_m = 1.5 \pm 0.5$ mM $n_H = 0.9 \pm 0.2$

[a] Variation on kinetic parameters are given as S.E.M. J_{max} is the maximal flux, K_m the Michaelis–Menten constant, n_H the Hill-constant, and P_{app} is the apparent permeability.

3.2. *Selection and structural properties of tripeptidomimetics*

A five principal component analysis (PCA) model was developed based on the 6859 tripeptidomimetics and their structural properties represented by the VolSurf descriptors. From this model the PCA score plots (Fig. 4, I and II) and PCA loading plot (Fig. 4, III) were extracted. The seven tripeptidomimetics included in the study were selected from different areas of the structural property space spanned both by the first and second principal component and the second and third principal component (Fig. 4, I and II). Hence, the compounds were selected in order to cover the variation in the structural properties of this type of tripeptidomimetics.

The VolSurf descriptors described the structural properties of the tripeptidomimetics. Compounds situated in different areas of the PCA score plots (Fig. 4, I and II) are predominantly described by the descriptors represented in the same area of the PCA loading plot (Fig. 4, III). Thus, the diversity in structural properties of the tripeptidomimetics was recognized by the differences in influential descriptors. In more details, DΨRΨE (Fig. 4, I. Grey full line circle) was mainly described by descriptors representing hydrophilic properties (Fig. 4, III. Grey full

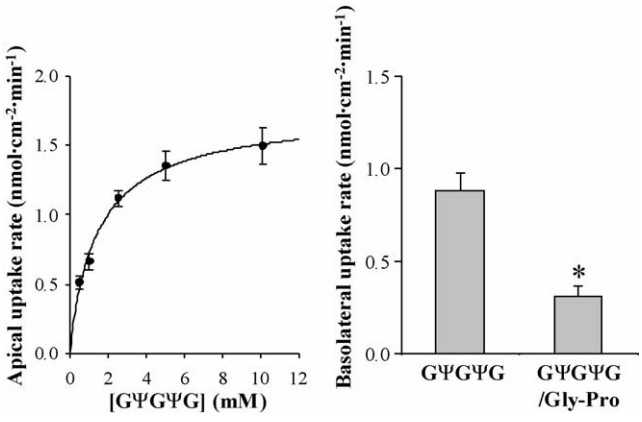

Fig. 3 – Left: Apical uptake of GΨGΨG (N = 6). Right: Basolateral uptake of 20 mM GΨGΨG in absence and presence of 20 mM Gly-Pro (N = 6), * significant difference ($p > 0.05$). Data are given as mean ± S.E.M.

line circle); KΨWΨR and NΨFΨW (Fig. 4, I, large punctuated circle) were primarily described by size, shape and hydrophobic properties (Fig. 4, III, large punctuated circle); GΨGΨG, GΨGΨL, and GΨFΨG (Fig. 4, I, black full line small circle) were mainly described by hydrophilic properties in the sense of the balance between the centre of the mass in the molecule and the centre of the polar region of the molecule (Fig. 4, III, black full line small circle); GΨEΨW (Fig. 4, I, small punctuated circle) was predominantly described by descriptors representing the balance between the centre of the mass in the molecule and the centre of the hydrophobic region of the molecule (Fig. 4, I, small punctuated circle) (for detailed descriptor definitions see ref. VolSurf Manual (2005) and Cruciani et al., 2000).

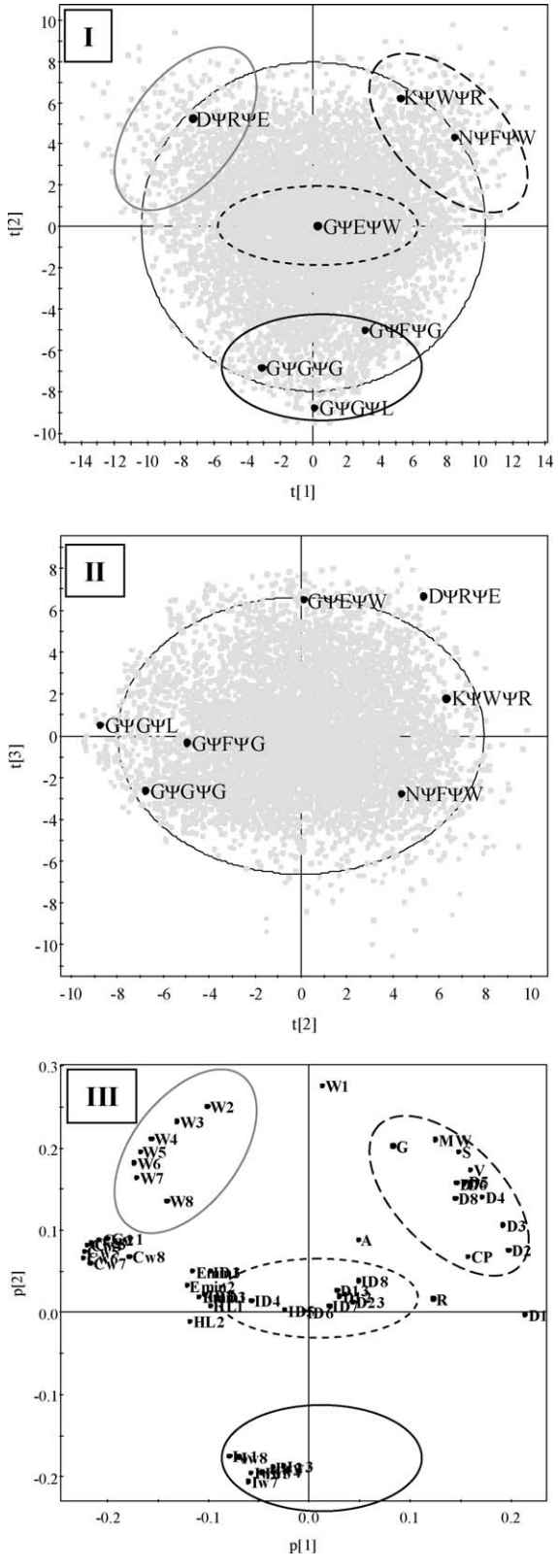

Fig. 4 – (I) PCA score plot where *t*[1] and *t*[2] is the first and second principal component, respectively. (II) PCA score plot where *t*[2] and *t*[3] is the second and third principal component, respectively. The principal components were extracted from the five principle component model. The obtained regression coefficient R^2 (goodness of model fit) and the predictive correlation coefficient Q^2 (goodness of predictions by the model) was 0.78 and 0.75, respectively. The large circle (black full line) is the 95% confidence interval. The first, second, and third principal component explained 33%, 19%, and 13%, respectively, of the structural variation derived from VolSurf descriptors of the tripeptidomimetics. The grey and black dots represent the 6859 *N*-methyl amide tripeptidomimetics. (III) PCA loading plot of the loadings of the first (*p*[1]) and second (*p*[2]) principal component. Variables important for the description of a tripeptidomimetic are located in the same area of the loading plot as the tripeptidomimetic in the score plot. Punctuated black circles and full line grey- and black circles (I and III) enclose tripeptidomimetic and corresponding influential descriptors.

3.3. *Affinity and transepithelial transport of the tripeptidomimetics*

The affinities of the seven tripeptidomimetics and their corresponding tripeptides are given in Table 2. High apparent affinity ($K_{i,\,app} < 0.5$ mM) was seen for the tripeptides GGL, GFG, and NFW. GGG, GEW, DRE, GΨGΨG, GΨGΨL, and NΨFΨW had medium apparent affinities (0.5 mM < $K_{i,app}$ < 5 mM). The introduction of *N*-methyl amide bioisosteres lowered the affinity for hPEPT1 of all tripeptidomimetics compared to the corresponding tripeptides, and it abolished the affinity in the case of GΨFΨG, KΨWΨR, GΨEΨW, and DΨRΨE (Table 2).

The AP to BL transepithelial transport at 2 mM was determined for the three tripeptidomimetics with affinity for hPEPT1, i.e. GΨGΨG, GΨGΨL, and NΨFΨW and for GΨFΨG with no affinity for hPEPT1 (Fig. 5). The transport was also measured in presence of 20 mM Gly-Pro to determine the contribution of hPEPT1-mediated transport to the overall transepithelial transport of the tripeptidomimetics.

The transport across Caco-2 cell monolayers of GΨGΨG was significantly higher than the transport of GΨGΨL, NΨFΨW, and GΨFΨG. The transepithelial transport of GΨGΨL was significantly higher than the transport of NΨFΨW and GΨFΨG, where the transport of NΨFΨW was significantly higher than the transport of GΨFΨG.

The transport of the tripeptidomimetics with affinity for hPEPT1 could be significantly inhibited by 20 mM Gly-Pro. This inhibitable component accounted for approximately 96% and 35% of the total transport of GΨGΨG and NΨFΨW, respectively,

Table 2 – Apparent K_i-values ($K_{i,app}$) for hPEPT1 of tripeptides/-mimetics measured as inhibition of [^{14}C]Gly-Sar uptake in Caco-2 cells

Tripeptide/-mimetic			$K_{i,app}$ (mM)[a]
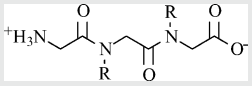	R=H	GGG	0.77 ± 0.04[b]
	R=CH$_3$	GΨGΨG	1.6 ± 0.1[b]
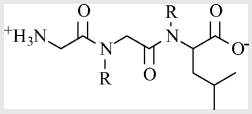	R=H	GGL	0.29 ± 0.002[b]
	R=CH$_3$	GΨGΨL	4.0 ± 1.2
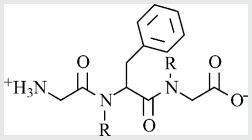	R=H	GFG	0.39 ± 0.004[b]
	R=CH$_3$	GΨFΨG	NA[c]
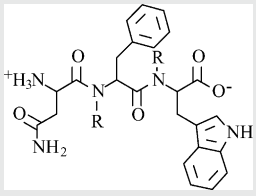	R=H	NFW	0.19 ± 0.003[b]
	R=CH$_3$	NΨFΨW	2.0 ± 0.7
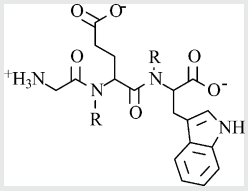	R=H	GEW	2.5 ± 1.2[b]
	R=CH$_3$	GΨEΨW	NA[c]
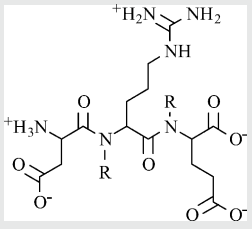	R=H	DRE	4.2 ± 2.5[b]
	R=CH$_3$	DΨRΨE	NA[c]
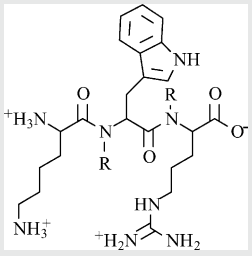	R=H	KWR	–[b,d]
	R=CH$_3$	KΨWΨR	NA[c]

[a] $K_{i,app}$ values are given as mean ± S.E.M.
[b] Data from Andersen et al. (2006).
[c] NA = No affinity.
[d] KWR was excluded from the affinity study as less than 90% of the compound was intact after 5 min.

while the transport of GΨGΨL was totally inhibited by Gly-Pro (Fig. 5).

To evaluate the effect of *N*-methylation on the stabilization of the tripeptides the amount of intact tripeptide/mimetic was measured on the AP side of the Caco-2 cells (Table 3). The amount of intact tripeptidomimetic present after 60 min

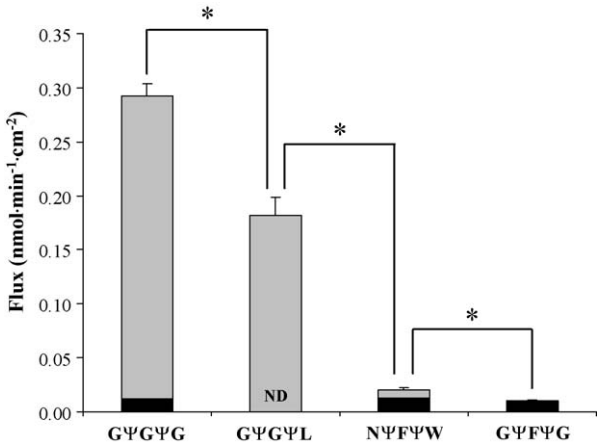

Fig. 5 – Transepithelial transport of 2 mM GΨGΨG (*N* = 8), GΨGΨL (*N* = 12), GΨFΨG (*N* = 9), and NΨFΨW (*N* = 3). Grey part of bar is the hPEPT1-mediated flux. Black part is the non-hPEPT1 mediated flux obtained in presence of 20 mM Gly-Pro. ND = No detectable transport. *Significant difference between groups ($p > 0.05$). Data are given as mean ± S.E.M.

Table 3 – Apparent degradation of tripeptide/-mimetic on the apical side of Caco-2 cell monolayers

	% Intact tripeptide/-mimetic after 60 min[a]
GGG[b]	91 ± 1
GΨGΨG[b]	94 ± 2
GGL[b]	79 ± 3
GΨGΨL	87 ± 3
GFG[b]	53 ± 4
GΨFΨG	84 ± 3
NFW[b]	57 ± 5
NΨFΨW	89 ± 6
GEW[b]	82 ± 0
GΨEΨW	92 ± 6
DRE[b]	71 ± 12
DΨRΨE	96 ± 2
KWR	21 ± 2
KΨWΨR	85 ± 11

[a] %Intact tripeptide/-mimetic are given as mean ± S.D. ($n = 3$).
[b] Data from Andersen et al. (2006).

was generally significantly higher than the amount of the corresponding tripeptide. However, because of the initially high stability of GGG only a slight increase in intact compound was observed after the *N*-methylation of this compound.

4. Discussion

A general evaluation of the affinity and transport of *N*-methyl amide tripeptidomimetics was performed in the present study. From all possible *N*-methylated tripeptides, seven structurally diverse compounds were selected and their affinity for and transepithelial transport via hPEPT1 of intact tripeptidomimetics were investigated and compared to the corresponding tripeptides.

4.1. *Transport mechanism of GΨGΨG*

The transport mechanism of the simplest *N*-methylated tripeptidomimetic, GΨGΨG, was investigated to initially explore the potential of this type of tripeptidomimetic as substrates for hPEPT1.

The predominant AP to BL transepithelial transport route for GΨGΨG was clearly active transport via hPEPT1. Thus, the paracellular and passive transepithelial transport could be considered negligible in the overall transport of GΨGΨG in the concentration range investigated. Furthermore, the transport across the BL membrane was suggested to occur partly via a yet unknown basolateral peptide transporter as the basolateral uptake of GΨGΨG could be partially inhibited by Gly-Pro (cf. Fig. 3) (Irie et al., 2004; Terada et al., 1999; Thwaites et al., 1993).

Considering GΨGΨG as a representative for the *N*-methyl amide tripeptidomimetics, it was concluded that *N*-methylated tripeptides might be transported by hPEPT1. Thus, a general evaluation of *N*-methylated tripeptides as substrates for hPEPT1 was initiated.

4.2. *Affinity of selected tripeptidomimetics*

The tripeptidomimetics GΨGΨG, NΨFΨW, and GΨGΨL showed affinity for hPEPT1 (cf. Table 2). However, the modification of the peptide bonds by *N*-methylation decreased the affinity for hPEPT1 compared to the affinities of the corresponding natural tripeptide (GGG, NFW, and GGL). Surprisingly, when the *N*-methyl amide isosteres were inserted into GFG, GEW, DRE, and KWR, the affinity for hPEPT1 was abolished.

In a recently proposed QSAR model partly based on tripeptides and β-lactam antibiotics it was suggested that the presence of a hydrogen bond donor in the second peptide bond of a tripeptide may have an unfavorable effect on the binding affinity for hPEPT1 (Biegel et al., 2005). Furthermore, the first general hPEPT1 substrate template proposed by Bailey et al. (2000) suggested that alkylation of the second amide bond was allowed. However, our results strongly indicate that the removal of hydrogen bond donors from the peptide bond of a tripeptide by *N*-methylation has an unfavorable effect on the affinity for hPEPT1. Still, the hPEPT1 transport protein to some extent accepts methylation of the peptide bonds as illustrated by GΨGΨG, NΨFΨW, and GΨGΨL. Yet, this acceptance is not general but depends on the structural properties of the side chains of the tripeptidomimetic as implied by the abolished affinity of GΨFΨG, GΨEΨW, DΨRΨE, and KΨWΨR. Thus, the affinities of this series of structurally very diverse compounds indicate that tripeptides with neutral side chains are more likely to bind to hPEPT1 after *N*-methylation of the peptide bonds than tripeptides with charged side chains. This observation corresponds well with the trend seen for affinities of natural tripeptides (Andersen et al., 2006).

In aqueous solution, tripeptides normally exist in a *trans* conformation around both peptide bonds. Based on studies of dipeptides, it has been suggested that the preferred conformation for binding to hPEPT1 is the *trans* conformation (Brandsch et al., 1998, 1999; Bailey et al., 2005). The introduction of *N*-methyl amide isosteres in tripeptides raises the possibility of a changed *cis* and *trans* conformation ratio, i.e. the combination of *cis*/*cis*, *trans*/*trans*, *cis*/*trans*, and *trans*/*cis* conformations of the peptide bonds. Thus, a change in the isomeric ratio of the tripeptidomimetics may decrease the concentration of the compound species adopting *trans*/*trans* conformation, which is assumed to be the conformation that binds to hPEPT1. Hence, the change in isomeric ratio may lead to an underestimation of the K_i-value of the binding compound specie. However, in the present evaluation of *N*-methylation as a general approach for stabilizing tripeptides and retain affinity for and transport via hPEPT1, it is the apparent K_i-values ($K_{i,app}$) which should be assessed. When determining the apparent affinity, the isomeric ratio is not taken into account. Moreover, the $K_{i,app}$-values are more representative of what may occur in an *in vivo* situation than K_i-values of the binding *trans*/*trans* conformation, assuming that the binding process is faster than the conversion of the *cis*/*cis*, *cis*/*trans*, or *trans*/*cis* conformations of the peptide bonds to the binding *trans*/*trans* form.

4.3. *Stability and transepithelial transport of selected tripeptidomimetics*

The *N*-methylations were introduced into the tripeptides to increase their stability. The stabilizing effect, at least *In vitro*, was observed by the increased amounts of intact tripeptidomimetics when applied to Caco-2 cells compared to the amount of the corresponding intact tripeptides (cf. Table 3).

Our strategy was to combine both stability and transport properties. Therefore, the transepithelial transport of GΨGΨG, NΨFΨW, and GΨGΨL, which had affinity for hPEPT1, was investigated to evaluate their possible translocation via hPEPT1 and subsequent ability to be effluxed across the basolateral membrane of Caco-2 cells. Furthermore, the transport of GΨFΨG, which was shown to have no affinity for hPEPT1, was investigated as a negative control.

The transepithelial transport of GΨGΨG, NΨFΨW, and GΨGΨL could be significantly inhibited by 20 mM Gly-Pro (cf. Fig. 5). In accordance with the lacking affinity of GΨFΨG, the transport of this compound could not be inhibited by Gly-Pro.

Thus, the tripeptidomimetics with affinity for hPEPT1 were also translocated by the transporter and subsequently effluxed across the basolateral membrane. Surprisingly, the flux of GΨGΨL with a low affinity ($K_{i,app}$ = 4.0 mM) for hPEPT1 was larger than the flux seen for NΨFΨW ($K_{i,app}$ = 2.0 mM) with a medium affinity for hPEPT1. This may indicate that the apparent affinities obtained as inhibition of the [^{14}C]Gly-Sar uptake are not predictive for the apical hPEPT1 translocation process. Alternatively, it could imply that the rate-limiting step in the transepithelial transport of GΨGΨL and NΨFΨW may not be the apical translocation via hPEPT1, but presumably the transport across the basolateral membrane.

5. Conclusion

The present investigation revealed that the *N*-methyl amide isostere is not generally applicable as a peptide bond replacement in a tripeptide, when the intension is to both increase stability and retain affinity and transport via hPEPT1 of the compound. Increased stability was seen for all tripeptides;

however, affinity for hPEPT1 did strongly depend on the structural properties of the side chains. GΨGΨG, NΨFΨW, and GΨGΨL had affinity for hPEPT1 and hPEPT1-mediated transport across Caco-2 cell monolayers. Thus, it was implied that *N*-methylated tripeptides with neutral side chains are more likely to be substrates for hPEPT1 than *N*-methylated tripeptides with charged side chains.

This *In vitro* evaluation indicated that the *N*-methyl amide isostere approach for increasing bioavailability of tripeptidomimetic drug candidates is only possible for a limited number of compounds where the overall structural properties of the tripeptide facilitates retention of affinity for and transport via hPEPT1.

We therefore suggest that future studies focus on development of more generally applicable amide bond isosteres in order to maintain suitable metabolic and intestinal permeability profiles of tripeptidomimetic drug candidates.

Acknowledgements

The Danish Medicinal Council supported this work (Project Grant #22-03-0274). Zealand Pharma A/S financially supported this work via the Drug Research Academy, Danish University of Pharmaceutical Sciences, Copenhagen, Denmark. Partly funding was achieved from the BioSim workpackage 15 funded by the European Commission (BioSim NoE LSH-CT-005137). The HPLC system was co-funded by the Hørslev Foundation. The technical assistance of Bettina Dinitzen and Susanne Nørskov Sørensen is highly valued. Peter Elm and Karina Thorn performed excellent synthesis assistance. We appreciate the support by Tripos Associates and Gabriele Cruciani regarding the access to Sybyl and VolSurf, respectively.

REFERENCES

Addison, J.M., Burston, D., Payne, J.W., Wilkinson, S., Matthews, D.M., 1975. Evidence for active transport of tripeptides by hamster jejunum *In vitro*. Clin. Sci. Mol. Med. 49, 305–312.

Andersen, R., Jørgensen, F.S., Olsen, J., Våbenø, J., Thorn, K., Nielsen, C.U., Steffansen, B., 2006. Development of a QSAR model for binding of tripeptides and tripeptidomimetics to the human intestinal di-/tri-peptide transporter hPEPT1. Pharm. Res. 23, 483–492.

Bailey, P.D., Boyd, C.A., Bronk, J.R., Collier, I.D., Meredith, D., Morgan, K.M., Temple, C.S., 2000. How to make drugs orally active: a substrate template for peptide transporter PepT1. Angew. Chem. Int. Ed. Engl. 39, 505–508.

Bailey, P.D., Boyd, C.A.R., Collier, I.D., Kellett, G.L., Meredith, D., Morgan, K.M., Pettecrew, R., Price, R.A., 2005. Probing dipeptide *trans/cis* stereochemistry using pH control of thiopeptide analogues, and application to the PepT1 transporter. Org. Biomol. Chem. 3, 4038–4039.

Biegel, A., Gebauer, S., Hartrodt, B., Brandsch, M., Neubert, K., Thondorf, I., 2005. Three-dimensional quantitative structure-activity relationship analyses of β-lactam antibiotics and tripeptides as substrates of the mammalian H^+/peptide cotransporter PEPT1. J. Med. Chem. 48, 4410–4419.

Brandsch, M., Knutter, I., Thunecke, F., Hartrodt, B., Born, I., Borner, V., Hirche, F., Fischer, G., Neubert, K., 1999. Decisive structural determinants for the interaction of proline derivatives with the intestinal H^+/peptide symporter. Eur. J. Biochem. 266, 502–508.

Brandsch, M., Thunecke, F., Kullertz, G., Schutkowski, M., Fischer, G., Neubert, K., 1998. Evidence for the absolute conformational specificity of the intestinal H^+/peptide symporter, PEPT1. J. Biol. Chem. 273, 3861–3864.

Bretschneider, B., Brandsch, M., Neubert, R., 1999. Intestinal transport of β-lactam antibiotics: Analysis of the affinity at the H^+/peptide symporter (PEPT1), the uptake into Caco-2 cell monolayers and the transepithelial flux. Pharm. Res. 16, 55–61.

Cheng, Y., Prusoff, W.H., 1973. Relationship between the inhibition constant (K_I) and the concentration of inhibitor which causes 50% inhibition (I_{50}) of an enzymatic reaction. Biochem. Pharmacol. 22, 3099–3108.

Cruciani, G., Crivori, P., Carrupt, P.A., Testa, B., 2000. Molecular fields in quantitative structure-permeation relationships: The VolSurf approach. J. Mol. Struct. THEOCHEM. 503, 17–30.

Daniel, H., Morse, E.L., Adibi, S.A., 1992. Determinants of substrate affinity for the oligopeptide/H^+ symporter in the renal brush border membrane. J. Biol. Chem. 267, 9565–9573.

Dantzig, A.H., 1998. Oral absorption of β-lactams by intestinal peptide transport proteins. Adv. Drug Deliver. Rev. 23, 63–76.

Doring, F., Walter, J., Will, J., Focking, M., Boll, M., Amasheh, S., Clauss, W., Daniel, H., 1998. Delta-aminolevulinic acid transport by intestinal and renal peptide transporters and its physiological and clinical implications. J. Clin. Invest. 101, 2761–2767.

Enjoh, M., Hashimoto, K., Arai, S., Shimizu, M., 1996. Inhibitory effect of arphamenine A on intestinal dipeptide transport. Biosci. Biotechnol. Biochem. 60, 1893–1895.

Friedrichsen, G.M., Nielsen, C.U., Steffansen, B., Begtrup, M., 2001. Model prodrugs designed for the intestinal peptide transporter. A synthetic approach for coupling of hydroxy-containing compounds to dipeptides. Eur. J. Pharm. Sci. 14, 13–19.

Ioudina, M., Uemura, E., 2003. A three amino acid peptide, Gly-Pro-Arg, protects and rescues cell death induced by amyloid beta-peptide. Exp. Neurol. 184, 923–929.

Irie, M., Terada, T., Okuda, M., Inui, K., 2004. Efflux properties of basolateral peptide transporter in human intestinal cell line Caco-2. Pflugers Arch. 449, 186–194.

Jia, J., Lu, R., Qiu, S., Li, H., Che, X., Zhao, P., Jin, M., Yang, H., Lin, G., Yao, Z., 2005. Preliminary investigation of the inhibitory effects of the tyroservaltide (YSV) tripeptide on human hepatocarcinoma BEL-7402. Cancer Biol. Ther. 4, 993–997.

Lange, U.E., Baucke, D., Hornberger, W., Mack, H., Seitz, W., Hoffken, H.W., 2003. D-Phe-Pro-Arg type thrombin inhibitors: unexpected selectivity by modification of the P1 moiety. Bioorg. Med. Chem. Lett. 13, 2029–2033.

Liang, R., Fei, Y.J., Prasad, P.D., Ramamoorthy, S., Han, H., Yang, F.T., Hediger, M.A., Ganapathy, V., Leibach, F.H., 1995. Human intestinal H^+/peptide cotransporter. Cloning, functional expression, and chromosomal localization. J. Biol. Chem. 270, 6456–6463.

Minami, H., Daniel, H., Morse, E.L., Adibi, S.A., 1992. Oligopeptides: mechanism of renal clearance depends on molecular structure. Am. J. Physiol. 263, F109–F115.

Nielsen, C.U., Amstrup, J., Steffansen, B., Frokjaer, S., Brodin, B., 2001a. Epidermal growth factor inhibits glycylsarcosine transport and hPepT1 expression in a human intestinal cell line. Am. J. Physiol. Gastrointest. Liver Physiol. 281, G191–G199.

Nielsen, C.U., Andersen, R., Brodin, B., Frokjaer, S., Taub, M.E., Steffansen, B., 2001b. Dipeptide model prodrugs for the intestinal oligopeptide transporter. Affinity for and transport

via hPepT1 in the human intestinal Caco-2 cell line. J. Control. Rel. 76, 129–138.
Sleisenger, M.H., Burston, D., Dalrymple, J.A., Wilkinson, S., Mathews, D.M., 1976. Evidence for a single common carrier for uptake of a dipeptide and a tripeptide by hamster jejunum *In vitro*. Gastroenterology 71, 76–81.
Still, W.C., Kahn, M., Mitra, A.K., 1978. Rapid chromatographic technique for preparative seperations with moderate resolution. J. Org. Chem. 43, 2923–2925.
Terada, T., Sawada, K., Saito, H., Hashimoto, Y., Inui, K., 1999. Functional characteristics of basolateral peptide transporter in the human intestinal cell line Caco-2. Am. J. Physiol. 276, G1435–G1441.
Thwaites, D.T., Brown, C.D., Hirst, B.H., Simmons, N.L., 1993. Transepithelial glycylsarcosine transport in intestinal Caco-2 cells mediated by expression of H^+-coupled carriers at both apical and basal membranes. J. Biol. Chem. 268, 7640–7642.
Våbenø, J., Nielsen, C.U., Ingebrigtsen, T., Lejon, T., Steffansen, B., Luthman, K., 2004a. Dipeptidomimetic ketomethylene isosteres as pro-moieties for drug transport via the human intestinal di-/tripeptide transporter hPEPT1: Design, synthesis, stability, and biological investigations. J. Med. Chem. 47, 4755–4765.
Våbenø, J., Lejon, T., Nielsen, C.U., Steffansen, B., Chen, W., Ouyang, H., Borchardt, R.T., Luthman, K., 2004b. Phe-Gly dipeptidomimetics designed for the di-/tri-peptide transporters PEPT1 and PEPT2: Synthesis and biological investigations. J. Med. Chem. 47, 1060–1069.
Yao, Z., Lu, R., Jia, J., Zhao, P., Yang, J., Zheng, M., Lu, J., Jin, M., Yang, H., Gao, W., 2005. The effect of tripeptide tyroserleutide (YSL) on animal models of hepatocarcinoma. Peptides., doi:10.1016/j.peptides.2005.02.026.
VolSurf Manual (VolSurf v4.1.3) Molecular Discovery Ltd. http://www.moldiscovery.com/soft_volsurf.php (accessed 22/11/05).